Inorg. Chem. **2004**, *43*, 8061–8071

Structure and Bonding of the Vanadium(III) Hexa-Aqua Cation. 2. Manifestation of Dynamical Jahn–Teller Coupling in Axially Distorted Vanadium(III) Complexes

Philip L. W. Tregenna-Piggott* and Graham Carver

Department of Chemistry, University of Bern, Freiestrasse 3, CH-3000, Bern 9 Switzerland

Received May 31, 2004

Ground-state spin-Hamiltonian parameters, magnetic data, and electronic Raman spectra of hexacoordinate vanadium(III) complexes are calculated with consideration to the $({}^3A \oplus {}^3E) \otimes e$ vibronic interaction and compared to experimental data. It is shown that the zero-field-splitting of the ${}^3A_g$ (S_6) ground term may be reduced significantly by the dynamical Jahn–Teller effect, particularly when the π-anisotropy of the metal–ligand bonding interaction is significant, and the energy of the Jahn–Teller active vibration is comparable to the diagonal axial field. The dynamical Jahn–Teller effect may also give rise to a significant enhancement in the Raman intensity of overtones and higher harmonics of Jahn–Teller active vibrations, when the energies of these transitions fall in the proximity of intra-${}^3T_{1g}$ (O_h) electronic Raman transitions. A simple method of conducting vibronic coupling calculations is described, employing ligand field matrices generated by angular overlap model calculations, which may in principle be applied to any transition metal complex.

1. Introduction

Ever since the first unambiguous experimental evidence for the Jahn−Teller effect in the paramagnetic resonance spectra of copper fluorosilicate,[1] interest in the influence of Jahn−Teller coupling on the spin-Hamiltonian parameters of transition metal complexes has continued unabated. The vast majority of work in this area has focused on copper(II) complexes, as the $3d^9$ electronic configuration is relatively simple, a strong Jahn−Teller effect is expected, and copper(II) complexes are amenable to study by conventional EPR over a wide temperature range. Less attention has been devoted to non-Kramers ions: The ground-state zero-field-splittings are usually too large to permit the detection of the $\Delta M_s = \pm 1$ spin allowed transitions using conventional X-band EPR, and the additional complication of interelectronic repulsion increases the number of parameters required to describe the system. The lack of experimental data is now being rapidly redressed by the application of high-field multifrequency EPR (HFMF EPR),[2] inelastic neutron scattering (INS),[3] and far-infrared[4] techniques. Complexes of Mn(III),[2−6] Fe(II),[7,8] Cr(II),[9,10] Ni(II),[4,11] and V(III)[12−15] have been investigated, rekindling interest in the theoretical description of the electronic structure of non-Kramers ions.

* To whom correspondence should be addressed. E-mail: tregenna@iac.unibe.ch.

(1) Bleaney B.; Ingram, D. J. E. *Proc. Phys. Soc., London, Sect. A* **1950**, *63*, 408. Bleaney B.; Bowers, K. D. *Proc. Phys. Soc., London, Sect. A* **1952**, *65*, 667.
(2) Smith, G. M.; Riedi, P. C. *Electron Paramagn. Reson.* **2000**, *17*, 164−204.
(3) Basler, R.; Tregenna-Piggott, P. L. W.; Andres, H.; Dobe, C.; Gudel, H.; Janssen, S.; McIntyre, G. J. *J. Am. Chem. Soc.*, **2001**, *123*, 3377−3378.
(4) Vongtragool, S.; Gorshunov, B.; Dressel, M.; Krzystek, J.; Eichhorn, D. M.; Telser, J. *Inorg. Chem.* **2003**, *42* (6), 1788−1790.
(5) Gatteschi, D.; Sorace, L.; Sessoli, R.; Barra, A. L. *Appl. Magn. Reson.* **2001**, *21*, 299−310.
(6) Krzystek, J.; Yeagle, G. J.; Park, J.-H.; Britt, R. D.; Meisel, M. W.; Brunel, L.-C.; Telser, J. *Inorg. Chem.* **2003**, *42*, 4610−4618.
(7) Knapp, M. J.; Krzystek, J.; Brunel, L.-C.; Hendrickson, D. N. *Inorg. Chem.* **2000**, *39*, 281−288.
(8) Carver, G.; Tregenna-Piggott, P. L. W.; Barra, A.-L.; Neels, A.; Stride, J. A. *Inorg. Chem.* **2003**, *42*, 5771−5777.
(9) Telser, J.; Pardi, L. A.; Krzystek, J.; Brunel, L.-C. *Inorg. Chem.* **1998**, *37*, 5769.
(10) Dobe, C.; Tregenna-Piggott, P. L. W.; Mossin, S.; Weihe, H.; Janssen, S.; *Chem. Phys. Lett.* **2002**, *362*, 387−396.
(11) Krzystek, J.; Park, J.-H.; Meisel, M. W.; Hitchman, M. A.; Stratemeier, H.; Brunel, L.-C.; Telser, J. *Inorg. Chem.* **2002**, *41* (17), 4478−4487.
(12) Tregenna-Piggott, P. L. W.; Weihe, H.; Bendix, J.; Barra, A.-L.; Güdel, H.-U. *Inorg. Chem.* **1999**, *38*, 5928.
(13) Accompanying paper: Tregenna-Piggott, P. L. W.; Spichiger, D.; Carver, G.; Frey, B.; Meier, R.; Weihe, H.; Cowan, J.; McIntyre, G.; Zahn, G.; Barra, A.-L. *Inorg. Chem.* **2004**, *43*, 8049−8060.
(14) Tregenna-Piggott, P. L. W.; Best, S. P.; Güdel, H. U.; Weihe, H.; Wilson, C. C. *J. Solid State Chem.* **1999**, *145*, 460.
(15) Krzystek, J.; Fiedler, A. T.; Sokol, J. J.; Ozarowski, A.; Zvyagin, S. A.; Brunold, T- C.; Long, J. R.; Brunel, L.-C.; Telser, J. *Inorg. Chem.* **2004**, *43*, 5645.

10.1021/ic049291t CCC: $27.50
Published on Web 11/03/2004

In this paper, the effect of dynamical Jahn−Teller coupling on the energies and magnetic properties of the low-lying vibronic states of a six-coordinate, trigonally distorted d^2 complex is examined. Motivation was provided by recent spectroscopic measurements on the vanadium(III) hexa-aqua cation in a range of β alums of the type $M^{I}V(SO_4)_2 \cdot 12X_2O$ ($M^{I}VSX$) and $Cs[Ga:V](SO_4)_2 \cdot 12X_2O$ (Cs[Ga:V]SX) where M^{I} = Cs or Rb, and X = hydrogen or deuterium, as well the guanidinium salt $GuV(SO_4)_2 \cdot 6H_2O$ (GuVSH).[12−14] The need to consider the vibrational coordinates is evinced by the anomalous band profile of the $^3A_g \rightarrow {}^3E_g$ (S_6) electronic Raman transition, which shows great sensitivity to deuteriation.[16]

The importance of Jahn−Teller coupling, in determining the electronic structure of compounds containing the vanadium(III) cation, has been demonstrated by optical measurements on vanadium(III) doped Al_2O_3 ($V^{3+}:Al_2O_3$).[17−19] The fine structure of the ^3A_g ($^3T_{1g}$) $\rightarrow {}^3T_{2g}$ zero-phonon transition is indicative of a strong dynamical Jahn−Teller effect, which can be explained in the theoretical framework of Ham,[20] treating the trigonal field and spin−orbit coupling as subsequent perturbations to the Jahn−Teller interaction.[21] The influence of dynamical Jahn−Teller coupling on the ground-state spin-Hamiltonian parameters of the same system has been discussed by Pontnau and Adde,[22] as well as Abou-Ghantous and Bates.[23] Both sets of authors incorporated various reduction factors multiplying orbital operators within an effective Hamiltonian. The reduction factors were not evaluated explicitly, however, and the analysis of Abou-Ghantous and Bates is not consistent with subsequent luminescence measurements enabling a direct measure of the diagonal trigonal field,[24] suggesting that the degree to which Jahn−Teller coupling governs the ground-state zero-field-splitting should be re-evaluated.

A number of notable disquisitions on Jahn−Teller coupling are now available, in which the physics underlying the phenomena is described in depth.[25−30] The perturbation theory approach, commonly adopted in vibronic coupling calculations, is accompanied in this work by numerical ($^3A \oplus {}^3E$) $\otimes$ e calculations, which may be readily adopted by nonspecialists in the field. By drawing on the wealth of experimental data now available for the vanadium(III) alums, we are able to quantify vibronic reduction factors and other manifestations of dynamic Jahn−Teller coupling, all too often neglected by inorganic chemists.

2. The Hamiltonian for the System

The Hamiltonian is written as the sum

$$\hat{H} = \hat{H}_{LF+ER} + \hat{H}_{SO} + \hat{H}_{Zee} + \hat{H}_{ph} + \hat{H}_{JT} \qquad (1)$$

where the first term includes the effect of both the ligand field and interelectronic repulsion, and the subsequent terms designate spin−orbit coupling, Zeeman, phonon, and Jahn−Teller contributions to the energy, respectively.

Calculations are presented employing two different electronic basis sets. Confining our attention to the $^3T_{1g}$ (O_h) ground term, the electronic orbital wave functions relative to the 3-fold axis, are defined in terms of $|L, M_L\rangle$, as[31]

$$|0\rangle = (1 + c_{LF}{}^2)^{-1/2}[-2/3|3, 0\rangle - \sqrt{5/18}(|3, 3\rangle - |3, -3\rangle) + c_{LF}|1, 0\rangle],$$
$$|\pm A\rangle = (1 + c_{LF}{}^2)^{-1/2}[\pm\sqrt{5/6}|3, \pm 2\rangle + \sqrt{1/6}|3, \mp 1\rangle + c_{LF}|1, \mp 1\rangle] \qquad (2)$$

where c_{LF} is a coefficient describing the degree of $^3T_{1g}$(F), $^3T_{1g}$(P) mixing, defined in terms of the octahedral splitting parameter, Δ_o, and the Racah parameter B.[31] In the weak field limit $c_{LF} = 0$, and in the strong field limit $c_{LF} = -1/2$. The orbital angular momentum operators can then be evaluated as functions of the parameter A, where $A = (1.5 - c_{LF}{}^2)/(1 + c_{LF}{}^2)$. The orbital wave functions are combined with the three spin functions, $|S, M_s\rangle = |1, 1\rangle$, $|1, -1\rangle$ and $|1, 0\rangle$ to form the 9 states of the $^3T_{1g}$ (O_h) electronic basis set. The matrix representation of the terms $\hat{H}_{LF+ER} + \hat{H}_{SO} + \hat{H}_{Zee}$ in the complex $^3T_{1g}$ (O_h) trigonal basis is given in Table 1.

In the previous paper, EPR data were presented, affording the determination of the ground-state spin-Hamiltonian parameters to unprecedented precision, warranting the employment of a more general electronic basis set to model the data. This may be achieved either by further parametrization of the effective orbital angular momentum,[22,23,32,33] or enlarging the basis set to include all 45 states of the $3d^2$ configuration. To this end, we have made use of the program LIGFIELD,[34] which allows one to construct ligand field matrices, in the framework of the AOM. The principle of constructing the vibronic Hamiltonian rests on the Wigner−Eckart theorem, the application of which requires a knowledge of the transformation properties of the basis states. For the current problem, we require that the orbital components of the ground term transform as $\sim|+\rangle$, $\sim|-\rangle$, and $\sim|0\rangle$ in the complex trigonal basis. This may be achieved as follows: First, the Hamiltonian matrices $\hat{H}_{LF+ER} + \hat{H}_{SO} + \hat{H}_{Zee}$ are constructed in any given basis using the LIGFIELD

(16) Tregenna-Piggott, P. L. W.; Best, S. P. *Inorg. Chem.* **1996**, *35*, 5730.
(17) Scott, W. C.; Sturge, M. D. *Phys. Rev.* **1966**, *146*, 262.
(18) Stephens, P. J.; Lowe-Pariseau, M. *Phys. Rev.* **1968**, *171*, 322.
(19) Champagon, B.; Duvel, E. *J. Phys. C: Solid State Phys.* **1980**, *13*, 141.
(20) Ham, F. S. *Phys. Rev.* **1965**, *138*, A1727
(21) Stephens, P. J. *J. Chem. Phys.* **1969**, *51*, 1995.
(22) Pontnau, J.; Adde, R. *Phys. Rev. B* **1976,** *14*, 3778.
(23) Abou-Ghantous, M.; Bates, C. A. *J. Phys.* **1980**, *41*, L-263.
(24) Reber, C.; Güdel, H. U. *Chem. Phys. Lett.* **1989**, *154*, 425
(25) Bersuker I. B. *The Jahn−Teller Effect and Vibronic Interactions in Modern Chemistry*; Plenum Press: New York, 1984.
(26) Ham F. S. Jahn−Teller Effects in Electron Paramagnetic Resonance Spectra. In *Electron Paramagnetic Resonance*; Geshwind, S., Ed.; Plenum Press: New York, 1972.
(27) Kaplan, M. D.; Vekhter, B. G. *Co-operative phenomena in Jahn−Teller crystals*; Plenum Press: New York, 1995.
(28) Sturge, M. D. *Solid State Phys.* **1967**, 91.
(29) O'Brien, M. C. M. *Vibrational Spectra and Structure*; Durig, J. R., Ed.; Elsevier: Amsterdam, 1981; pp 321−394.
(30) Bersuker, I. B. *Chem. Rev.* **2001**, *101*, 1067−1114.
(31) Mabbs, F. E.; Collison, D. *Electron Paramagnetic Resonance of Transition Metal Compounds*; Elsevier: New York, 1992; p 334.
(32) Abraham, A.; Pryce, M. H. L. *Proc. R. Soc. London, Ser. A* **1951**, *205*, 135.
(33) Chakravarty, A. S. *Proc. R. Soc. London, Ser. A* **1959**, *74*, 711.
(34) Bendix, J. *Compr. Coord. Chem. II* **2004**, *2*, 673−676.

Table 1. Hamiltonian Matrix for the Ligand-Field, Spin−Orbit Coupling, and Zeeman Terms in a Complex $^3T_{1g}$ Trigonal Basis

	$\|A,1\rangle$	$\|A,-1\rangle$	$\|A,0\rangle$	$\|-A,1\rangle$	$\|-A,-1\rangle$	$\|-A,0\rangle$	$\|0,1\rangle$	$\|0,-1\rangle$	$\|0,0\rangle$
$\langle A,1\|$	$\beta B_z(kA+g_e)+\Delta/3+A\lambda$	0	$\beta g_e\sqrt{2}(B_x-iB_y)$	0	0	0	$-\beta kA/\sqrt{2}(B_x+iB_y)$	0	$-A\lambda$
$\langle A,-1\|$	0	$\beta B_z(kA-g_e)+\Delta/3-A\lambda$	$\beta g_e\sqrt{2}(B_x+iB_y)$	0	0	0	0	$-\beta kA/\sqrt{2}(B_x+iB_y)$	0
$\langle A,0\|$	$\beta g_e\sqrt{2}(B_x+iB_y)$	$\beta g_e\sqrt{2}(B_x-iB_y)$	$\beta B_z kA+\Delta/3$	0	0	0	0	$-A\lambda$	$-\beta kA/\sqrt{2}(B_x+iB_y)$
$\langle -A,1\|$	0	0	0	$\beta B_z(-kA+g_e)+\Delta/3-A\lambda$	0	$\beta g_e\sqrt{2}(B_x-iB_y)$	$-\beta kA/\sqrt{2}(B_x-iB_y)$	0	0
$\langle -A,-1\|$	0	0	0	0	$\beta B_z(-kA-g_e)+\Delta/3+A\lambda$	$\beta g_e\sqrt{2}(B_x+iB_y)$	0	$-\beta kA/\sqrt{2}(B_x-iB_y)$	$-A\lambda$
$\langle -A,0\|$	0	0	0	$\beta g_e\sqrt{2}(B_x+iB_y)$	$\beta g_e\sqrt{2}(B_x-iB_y)$	$-\beta B_z kA+\Delta/3$	$-A\lambda$	0	$-\beta kA/\sqrt{2}(B_x-iB_y)$
$\langle 0,1\|$	0	$-\beta kA/\sqrt{2}(B_x-iB_y)$	0	$-\beta kA/\sqrt{2}(B_x+iB_y)$	0	$-A\lambda$	$-\beta B_z g_e+-2\Delta/3$	0	$\beta g_e/\sqrt{2}(B_x-iB_y)$
$\langle 0,-1\|$	0	$-\beta kA/\sqrt{2}(B_x-iB_y)$	$-A\lambda$	0	$-\beta kA/\sqrt{2}(Bx+iB_y)$	0	0	$-\beta B_z g_e+-2\Delta/3$	$\beta g_e/\sqrt{2}(Bx+iB_y)$
$\langle 0,0\|$	$-A\lambda$	0	$-\beta kA/\sqrt{2}(B_x-iB_y)$	0	$-A\lambda$	$-\beta kA/\sqrt{2}(B_x+iB_y)$	$\beta g_e/\sqrt{2}(B_x+iB_y)$	$\beta g_e/\sqrt{2}(B_x-iB_y)$	$-2\Delta/3$

program. Next, the matrix $\hat{H}_{LF+ER}$ is diagonalized, and the eigenfunctions are used to construct the coefficient matrix for the unitary transformation

$$C_{LF+ER}{}^{\dagger}(\hat{H}_{LF+ER}+\hat{H}_{SO}+\hat{H}_{Zee})C_{LF+ER}=(\hat{H}_{LF+ER}+\hat{H}_{SO}+\hat{H}_{Zee})' \quad (3)$$

where $\hat{H}_{LF+ER}{}'$ is diagonal. The nine lowest-lying states now transform as the ^3E_g and ^3A_g components of the $^3T_{1g}$ (O_h) ground term. We require that the operators $\hat{L}_z$ and $\hat{S}_z$ be diagonal within the ^3E_g term. This is achieved by diagonalizing the matrix representation of $\hat{L}_z+\hat{S}_z$ operating within the ^3E_g term, and using the eigenvectors for the subsequent unitary transformation:

$$C_{\hat{L}_z+\hat{S}_z}{}^{\dagger}(\hat{H}_{LF+ER}+\hat{H}_{SO}+\hat{H}_{Zee})'C_{\hat{L}_z+\hat{S}_z}=(\hat{H}_{LF+ER}+\hat{H}_{SO}+\hat{H}_{Zee})'' \quad (4)$$

The states transforming as the orbital functions $\sim|+\rangle$, $\sim|-\rangle$, and $\sim|0\rangle$ may be identified by inspection of $\langle\hat{L}_z\rangle$. The M_s quantum number is identified by evaluating $\langle\hat{S}_z\rangle$.

The form of the vibronic Hamiltonian then follows from consideration of symmetry. We set out to show the general effect of vibronic coupling on the ground electronic structure of the vanadium(III) cation, without attempting to obtain quantitative agreement with experiment, and thus confine our attention to coupling with a single doubly degenerate vibration only. To first-order in the Jahn−Teller interaction, and ignoring anharmonicity, $\hat{H}_{ph}$ and $\hat{H}_{JT}$ may be written as

$$\hat{H}_{ph}=[0.5\hbar\omega(\hat{P}_x{}^2+\hat{P}_y{}^2+\hat{Q}_x{}^2+\hat{Q}_y{}^2)]\hat{U}_\tau$$

$$\hat{H}_{JT}=-\frac{A_1{}^{EE}}{\sqrt{2}}(\hat{Q}_+\hat{U}_-{}^{EE}+\hat{Q}_-\hat{U}_+{}^{EE})-\frac{A_1{}^{AE}}{\sqrt{2}}(\hat{Q}_+\hat{U}_-{}^{AE}+\hat{Q}_-\hat{U}_+{}^{AE}) \quad (5)$$

where $\hat{Q}_\pm={}^1/_2(\mp\hat{Q}_x-i\hat{Q}_y)$, and $\hat{Q}_x$, $\hat{Q}_y$ are the two-components of the degenerate e vibration of energy $\hbar\omega$. $A_1{}^{EE}$ and $A_1{}^{AE}$ are coefficients defining the $(^3A\oplus{}^3E)\otimes e$ vibronic coupling interaction. In the limit where $A_1{}^{EE}\rightarrow A_1{}^{AE}=A_1$, we may define the quantity $E_{JT}=A_1{}^2/2\hbar\omega$, which is the T $\otimes$ e Jahn−Teller stabilization energy. $\hat{U}_\tau$ is the unit matrix, and $\hat{U}_+{}^{EE}$, $\hat{U}_-{}^{EE}$, $\hat{U}_+{}^{AE}$, $\hat{U}_-{}^{AE}$ are electronic operators, connecting the orbital components of the $^3T_{1g}$ (O_h) ground term, constructed using the Clebsh−Gordan coefficients as listed by S. Sugano, Y. Tanabe, and H. Kamimura:[35]

$$\hat{U}_+{}^{EE}=\begin{pmatrix}0&0&0\\1&0&0\\0&0&0\end{pmatrix};\ \hat{U}_-{}^{EE}=\begin{pmatrix}0&-1&0\\0&0&0\\0&0&0\end{pmatrix};$$

$$U_+{}^{AE}=\begin{pmatrix}0&0&1\\0&0&0\\0&-1&0\end{pmatrix};\ \hat{U}_-{}^{AE}=\begin{pmatrix}0&0&0\\0&0&1\\-1&0&0\end{pmatrix} \quad (6)$$

where the orbital basis functions transform as $\sim|+\rangle$,

(35) Sugano, S.; Tanabe, Y.; Kamimura, H. *Multiplets of Transition Metal Ions In Crystals*; Academic Press: New York, 1970.

$\sim|-\rangle$, and $\sim|0\rangle$. $\hat{Q}_i$ and $\hat{P}_i$ are dimensionless operators, related to the observables for position and momentum, $\hat{q}_i$, $\hat{p}_i$ by[36]

$$\hat{Q}_i = \sqrt{\frac{\mu\omega}{\hbar}}\hat{q}_i \quad P_i = \frac{1}{\sqrt{\mu\hbar\omega}}\hat{p}_i \tag{7}$$

where μ is the reduced mass of the phonon mode.

The magnitudes of the vibronic coupling constants may be estimated by way of DFT[37−39] or AOM [40−43] calculations. For the $[V(OH_2)_6]^{3+}$ cation, coupling between the $^3T_{1g}(O_h)$ ground term and the ρ_τ twisting libration of water is expected to be prevalent, on the basis of an extensive experimental and theoretical study of the $[Ti(OH_2)_6]^{3+}$ cation.[43−48] The form of the twisting libration is depicted in Figure 5 of ref 45. In the β-alums, the librational modes of water coordinated to the tervalent cation are strongly coupled, occurring between ~750 and ~950 cm^{-1} in the hydrogenous salt, and between 550 and 700 cm^{-1} in the deuteriated salt.[49] Expressions formulated in the framework of the AOM by Bendix, commonly known in the trade as the Jespi equations, predict a complicated dependence of the values of the coupling constants on the geometric and bonding parameters.[43] Nevertheless, throughout this work, A_1^{EE} is set equal to A_1^{AE}. The approximation is convenient, as the number of parameters is reduced, and many of the quantities of interest vary linearly with E_{JT}. Electronic Raman data of the $[V(OH_2)_6]^{3+}$ cation in the GuVSH alum are indicative of dynamical Jahn−Teller coupling, with $E_{JT} \sim 300$ cm^{-1}.[69] The π-bonding in $[V(OH_2)_6]^{3+}$ is highly anisotropic,[13,14] and the linear splitting of the electronic states, along a given asymmetric coordinate, is predicted to diminish as the ligand becomes linearly ligating.[45] The degree of dynamical Jahn−Teller coupling is therefore minimal for the $[V(halide)_6]^{3-}$ complexes in the cubic elpasolites, where the $V(halide)_6$ framework is regular.[50] Coupling to the $\nu_2(VL_6)$ mode will increase, however, as the VL_6 framework becomes trigonally distorted. For the $Al_2O_3:Ti^{3+}$ system, we are able to reproduce the low energy vibronic spectrum,[51] setting $\hbar\omega$ to 239 cm^{-1},[52,53] and E_{JT} to 308 cm^{-1}. Similar values for the vibronic parameters are anticipated for $Al_2O_3:V^{3+}$. In the next section, calculations are presented with E_{JT} ranging from 0 to 350 cm^{-1}. We consider 350 cm^{-1} as the upper limit of E_{JT} to be expected for any given hexacoordinate homoleptic vanadium(III) complex.

The Hamiltonian was constructed as a matrix in a basis of products of the electronic states and the states of the $\{Q_x, Q_y\}$ harmonic oscillator of dimension $N = {}^1/_2(n_v + 1)(n_v + 2)$, up to the level n_v. The matrix was brought to diagonal form using a fast Lanczos diagonalization routine for real symmetric matrices. This meant a further doubling of the size of the original complex matrix. As is usual in this type of calculation, the size of the basis set was increased until adequate convergence of the low energy eigenvalues was achieved. For the present calculations, n_v was typically set to 16, resulting in matrices of dimensions 2754 and 13770 for calculations using the two electronic basis sets. The limited electronic basis in Table 1 was used to calculate electronic Raman spectra and the magnetic properties of the vanadium(III) cation. The ground-state spin-Hamiltonian parameters were calculated using both electronic bases.

The vibronic eigenfunctions of the Hamiltonian, Ψ, are expressed as linear combinations of the basis functions. For calculations using the electronic basis set given in Table 1, Ψ is expressed as

$$\Psi = \sum_i \sum_j \sum_{k+l=0}^{n_v} a_{ijkl}|\psi_i, M_{sj}, n_{xk}, n_{yl}\rangle \tag{8}$$

where ψ_i spans the three orbital components of the $^3T_{1g}$ ground term, and n_x and n_y are the quantum numbers of the harmonic oscillators.

(36) Cohen-Tannoudji, C.; Diu, B.; Laloe, F. *Quantum Mechanics*; John Wiley and Sons: New York, and Hermann: Paris, 1977; Vol. 1, Chapter V, p 488.
(37) Bruyndonckx, R.; Daul, C.; Manoharan, P. T.; Deiss, E. *Inorg. Chem.* **1997**, *36*, 4251.
(38) Kundu, T. K.; Bruyndonckx, R.; Daul, C.; Manoharan, P. T. *Inorg. Chem.* **1999**, *38*, 3931.
(39) Atanasov, M.; Schonherr, T. *THEOCHEM* **2002**, *592*, 79−93.
(40) Bacci, M. *Chem. Phys. Lett.* **1978**, *58*, 537.
(41) Bacci, M. *Chem. Phys.* **1979**, *40*, 237−244.
(42) Wissing, K.; Degen, J. *Mol. Phys.* **1998**, *95*, 51.
(43) Carver, G.; Bendix, J.; Tregenna-Piggott, P. L. W. *Chem. Phys.* **2002**, *282*, 245.
(44) Tregenna-Piggott, P. L. W.; Noble, C. J.; Pilbrow, J. R. *J. Chem. Phys.* **2000**, *113*, 3289−3301.
(45) Tregenna-Piggot, P. L. W.; Andres, H.-P.; McIntyre, G. J.; Best, S. P.; Wilson, C. C.; Cowan, J. *Inorg. Chem.* **2003**, *42*, 1350.
(46) Tregenna-Piggott, P. L. W.; O'Brien, M. C. M.; Pilbrow, J. R.; Güdel, H.-U.; Best, S. P.; Noble, C. *J. Chem. Phys.* **1997**, *107*, 8275.
(47) Tregenna-Piggott, P. L. W.; O'Brien, M. C. M.; Weihe H.; Güdel, H. U. *J. Chem. Phys.* **1998**, *109*, 2967.
(48) Tregenna-Piggott, P. L. W.; Güdel, H.-U. *Inorg. Chem.* **2001**, *40*, 5497.
(49) Best, S. P.; Beattie, J. K.; Armstrong, R. S. *J. Chem. Soc., Dalton Trans.* **1984**, 2611−2624.
(50) Reber, C.; Guedel, H. U.; Meyer, G.; Schleid, T.; Daul, C. A. *Inorg. Chem.* **1989**, *28*, 3249.
(51) Nelson, E. D.; Wong, J. Y.; Sturge, M. D. *Phys. Rev.* **1967**, *156*, 298.
(52) Gächter, B. F.; Koningstein, J. A. *J. Chem. Phys.* **1974**, *60*, 2003.
(53) Grinberg, M.; Mandelis, A.; Fjeldsted, K.; Othonos, A. *Phys. Rev. B* **1993**, *48*, 5922.
(54) Gächter, B. F. *J. Mol. Spectrosc.* **1976**, *63*, 1−22
(55) Mizusima, M. *Quantum Mechanics of Atomic Spectra and Atomic Structure*; W. A. Benjamin Inc. Press: New York, 1970; p 164.
(56) Sasaki, K.; Obata, Y. *J. Phys. Soc. Jpn.* **1970**, *28*, 1157.
(57) Ham, F. S. *J. Phys. Colloq.* **1971**, *32*, 952.
(58) Bhattacharyya, B. D. *Phys. Status Solidi B* **1975**, *71*, 427.
(59) Kugel, K. I.; Khomskii, D. I. *Usp. Fiz. Nauk* **1982**, *135*, 621.
(60) Borras-Almenar, D. D.; Ganurar, V. Ya; Kishinevskii, G. M.; Koronado, E.; Pali, A. V.; Tsukerblat, B. S. *Zh. Strukt. Khim.* **1994**, *35*, 28.
(61) Quade, C. R.; Mires, R. W.; Brumage, W. H.; Dorman, C. F. *J. Chem. Phys.* **2003**, *188*, 5506.
(62) Tregenna-Piggott, P. L. W. *Adv. Quantum Chem.* **2003**, *44*, 461.
(63) Dunbar, K. R.; Schelter, E. J.; Tsukerblat, B. S.; Ostrovsky, S. M.; Mirovitsky, V. Y.; Palii, A. V. *Polyhedron* **2003**, *22*, 2545−2556.
(64) van Vleck, J. H. *The Theory of Electric and Magnetic Susceptiblities*; Oxford University Press: London, 1932.
(65) Abragam, A.; Bleaney, B. *Electron Paramagnetic Resonance of Transition Metal Ions*; Clarendon Press: Oxford, 1970.
(66) Figgis, B. N.; Lewis, J.; Mabbs, F. *J. Chem. Soc.* **1960**, 2480.
(67) Figgis, B. N.; Lewis, J.; Mabbs, F.; Webb, G. A. *J. Chem. Soc.* **1966**, 1411.
(68) Ham, F. S. *Phys. Rev.* **1968**, *166*, 307.
(69) Spichiger, D.; Carver, G.; Dobe, C.; Bendix, J.; Tregenna-Piggott, P. L. W.; Meier, R.; Zahn, G. *Chem. Phys. Lett.* **2001**, *337*, 391.

3. Numerical Calculation of the Experimental Quantities

Calculations of the experimental quantities employing the restricted and full ligand field electronic bases were undertaken using programs written in FORTRAN 77 and MATHEMATICA 5.0, respectively. The FORTRAN program, in particular, is straightforward to use and is available from the corresponding author.

3.1. Raman Spectra. The electronic Raman cross section, I, for a transition from state Ψ to state Ψ', was calculated according to

$$I \propto E_s^{\,4} \exp\left(\frac{-E_i}{kT}\right)\langle\Psi|\hat{\alpha}_{\rho\sigma}|\Psi'\rangle\langle\Psi'|\hat{\alpha}_{\rho\sigma}|\Psi\rangle \qquad (9)$$

where E_s is the energy of the scattered radiation, E_i the energy of the state Ψ, and $\hat{\alpha}_{\rho\sigma}$ the component of the Raman polarizability tensor in the Cartesian laboratory frame. Tables relating the components of the Raman scattering in a Cartesian coordinate system to components which transform as irreducible representations of the scattering center in a given point, as well as linear combinations of spherical harmonics, have been dervied by Gächter for the 32 crystallographic point groups.[54] The spherical harmonics have the same symmetry properties as irreducible tensor operators, which may be written in terms of operator equivalents.[55] In the limit where $\Delta \gg A\lambda$, only those components transforming as linear combinations of $\hat{L}_+$, $\hat{L}_-$ result in significant intensity for transitions between the ^3A_g and ^3E_g terms,[69] in which case, the electronic matrix element may be expressed as

$$\langle\Psi|\hat{\alpha}_{\rho\sigma}|\Psi'\rangle = \sum_{k+l=0}^{n_v}\sum_{k'+l'=0}^{n'_v}(a_{i=A,kl}{}^{*}a'_{i=0,k',l'} + a_{i=0,kl}{}^{*}a'_{i=A,k'l'} + a_{i=-A,kl}{}^{*}a'_{i=0,k',l'} + a_{i=0,k,l}{}^{*}a'_{i=-A,k',l'})\delta_{kk'}\delta_{ll'} \qquad (10)$$

where we have omitted the expansion in terms of the electron spin. The calculated electronic Raman transitions were folded with a Gaussian bandwidth, with constant width across the whole spectrum.

3.2. Calculation of the Ground-State Spin-Hamiltonian Parameters. When $\Delta \gg A\lambda$, the magnetic behavior of the ^3A_g ground term may be conveniently described by the axial $S = 1$ spin-Hamiltonian:

$$\begin{array}{c|ccc} & |1\rangle & |-1\rangle & |0\rangle \\ \langle 1| & D/3 + g_{\parallel}\beta B_z & 0 & g_{\perp}\beta/\sqrt{2}(B_x - iB_y) \\ \langle -1| & 0 & D/3 - g_{\parallel}\beta B_z & g_{\perp}\beta/\sqrt{2}(B_x + iB_y) \\ \langle 0| & g_{\perp}\beta/\sqrt{2}\,(B_x + iB_y) & g_{\perp}\beta/\sqrt{2}(B_x - iB_y) & -2D/3 \end{array} \qquad (11)$$

From diagonalization of eq 11, closed form expressions for D, $g_{\parallel}$, and $g_{\perp}$ may be obtained. These parameters are then calculated from the eigenvalues of the three lowest lying states, obtained by the numerical procedure outlined above. For a given set of parameters, the calculation was performed a total of three times: once with the applied magnetic field B_0 set to zero, to yield D, the zero-field-splitting; once with $B_z = B_0$, $B_x = B_y = 0$, to yield $g_{\parallel}$; and once with $B_x = B_0$, $B_z = B_y = 0$, to yield $g_{\perp}$. B_0 was set to values small enough such that the calculated g values were independent of its magnitude.

3.3. Calculation of the Magnetic Properties. It has long been recognized, by specialists in the field, that dynamical Jahn−Teller coupling can have a profound effect on the magnetic properties of transition metal complexes,[46−48,56−63] though the phenomenon is yet to pervade the pages of modern treatises on magnetochemistry. The magnetic moment may be calculated either using the formalism of Ham[20,57,61] or from numerical diagonalization of the vibronic Hamiltonian,[46−48,62] as described here. The paramagnetic molar magnetic susceptibility was calculated according to the general expression[64]

$$\chi_M = \frac{N}{B_0}\frac{\sum_n\left(-\frac{dW_n}{dB_0}\right)\exp(-W_n/kT)}{\sum_n \exp(-W_n/kT)} \qquad (12)$$

where the sum is over the n eigenstates of the Hamiltonian (those with a significant population) and the derivatives are found using the Hellmann−Feynman theorem

$$\frac{dW_n}{dB_0} = \left\langle\Psi_n\left|\frac{d\hat{H}}{dB_0}\right|\Psi_n\right\rangle = \sum_i\sum_{i'}\sum_j\sum_{j'}\sum_{k+l=0}^{n_v}\sum_{k'+l'=0}^{n'_v} a_{ijkl}{}^{*}a_{i'j'k'l'} \left\langle\psi_i, M_{sj}\left|\frac{d\hat{H}}{dB_0}\right|\psi_{i'}, M_{sj'}\right\rangle\delta_{kk'}\delta_{ll'} \qquad (13)$$

This method allows the susceptibility at a given field to be calculated exactly from one diagonalization of the vibronic Hamiltonian. The quantity frequently reported as a function of temperature is the effective magnetic moment, which is related to χ_M by

$$\mu_{eff} = \left(\frac{3k}{N\beta^2}\right)^{1/2}(\chi_M T)^{1/2} \qquad (14)$$

4. Results and Discussion

4.1. Ligand-Field Description of the Ground-State Electronic Structure. The electronic structure and associated magnetic behavior of $^3T_{1g}$ (O_h) terms, in the absence of vibronic coupling, has been discussed by a host of authors[22,31−33,65−67] and shall be considered only briefly here. The Hamiltonian matrix arising from the terms $\hat{H}_{LF+ER} + \hat{H}_{SO}$ in Table 1 factors into three submatrices, which may be readily brought to diagonal form. In Figure 1a are shown the energies of the states as a function of Δ, where $A\lambda$ is set to 100 cm^{-1}. When $\Delta = 0$, the states transform the same way as those arising from the free-ion $^3P_{2,1,0}$ term, with the 5 levels of the $J = 2$ state lower lying. In the limit where $\Delta \gg A\lambda$, the spinor levels may be classified into groups comprising the ^3A_g and ^3E_g terms of the trigonal subgroup. The levels of the higher lying ^3E_g term are split to first-order by spin−orbit coupling, spanning an energy range of $\sim 2A\lambda$; the ^3A_g ground term is split to second-order by spin−

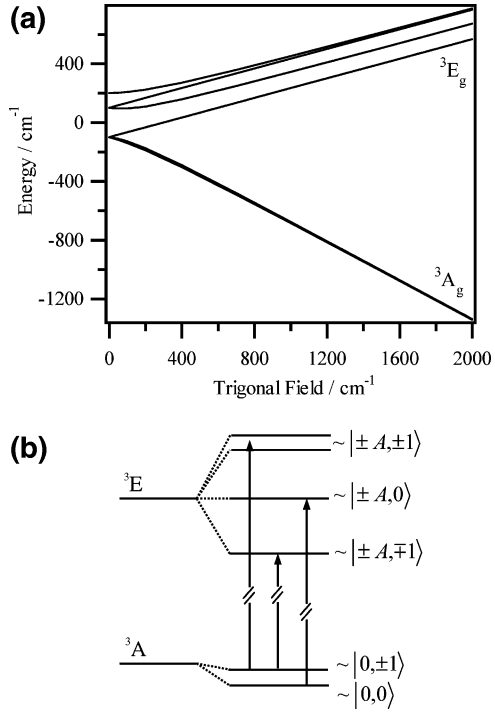

Figure 1. (a) Spinor-levels of the $^3T_{1g}$ (O_h) term as a function of Δ, calculated by diagonalization of the Hamiltonian matrix in Table 1, with $A\lambda$ set to 100 cm^{-1}. (b) Spinor levels of the $^3T_{1g}$ (O_h) ground term in the limit where $\Delta \gg A\lambda$. The arrows designate the allowed $^3A_g \rightarrow {}^3E_g$ (S_6) electronic Raman transitions, based on the $\Delta M_s = 0$ selection rule.

orbit coupling, with the two degenerate states for which $\langle \hat{S}_z \rangle \sim \pm 1$ raised in energy above the state for which $\langle \hat{S}_z \rangle \sim 0$, by an amount

$$D \approx (1/2)(S_0 - S_1 - A\lambda) \approx \frac{(A\lambda)^2(\Delta - A\lambda)}{\Delta(\Delta + A\lambda)} \approx \frac{(A\lambda)^2}{\Delta} \quad (15)$$

where

$$S_0 = \{(\Delta + A\lambda)^2 + 8A^2\lambda^2\}^{1/2} \quad S_1 = (\Delta^2 + 4A^2\lambda^2)^{1/2}$$

On evaluating the Zeeman energy as a perturbation, we find

$$g_{\|} = \frac{g_e - kA\delta^2}{1 + \delta^2} \approx 2 - (2 + kA)\delta^2$$

$$g_{\perp} = \frac{g_e + 2\delta\epsilon - kA(\delta + \epsilon)}{\{(1 + 2\epsilon^2)(1 + \delta^2)\}^{1/2}} \approx 2 - 2kA\delta - \delta^2 \quad (16)$$

where

$$\delta = \frac{S_1 - \Delta}{2A\lambda} \approx A\lambda/\Delta \quad \epsilon = \frac{S_0 - \Delta - A\lambda}{4A\lambda} \approx A\lambda/\Delta$$

The theory predicts a first-order deviation from the spin-only value for $g_{\perp}$, and a second-order deviation for $g_{\|}$. For the $[V(OH_2)_6]^{3+}$ cation in the β-alums, $\Delta = 1918$ cm^{-1} and $A = 1.414$ based on electronic Raman[16] and UV−vis absorption spectra.[13] Setting λ to 76 cm^{-1}, the ground-state spin-Hamiltonian parameters are evaluated as $D = +5.3375$ cm^{-1}, $g_{\|} = 1.9922$, $g_{\perp} = 1.8650$.

Figure 1b shows the splitting of the trigonal components of the $^3T_{1g}(O_h)$ term to first-order by spin−orbit coupling. The labels indicate the corresponding zeroth order wave functions. The arrows designate the allowed $^3A_g \rightarrow {}^3E_g$ electronic Raman transitions, based on the $\Delta M_s = 0$ selection rule. Three transitions of roughly equal intensity are expected, with an energy spacing $\sim A\lambda$.

For vanadium(III) complexes, spin−orbit coupling is very much smaller than both interelectronic repulsion and the octahedral ligand field splitting parameter 10Dq. There is little change in the calculated electronic Raman spectrum and magnetic susceptibility when the electronic basis is expanded to include all terms arising from the d^2 configuration. By comparison, EPR measurements afford a more exact characterization of the electronic structure. Spin−orbit coupling between the free-ion terms is evinced in a greater deviation of $g_{\|}$ from the spin-only value. Using the geometry of the $[V(OH_2)_6]^{3+}$ cation and the parameters $B = 644$, $C = 2960$, $e_{\sigma} = 6950$, $e_{\pi\perp} = 930$, $e_{\pi\|} = 0$, $\zeta = 174$ cm^{-1}, and $k = 0.88$ as input into the program LIGFIELD,[34] the following spin-Hamiltonian parameters are calculated: $D = +5.3162$ cm^{-1}, $g_{\|} = 1.9527$, $g_{\perp} = 1.8591$.

4.2. Effect of Jahn−Teller Coupling on the Ground-State Spin-Hamiltonian Parameters. In a series of seminal articles, Ham showed that dynamical Jahn−Teller coupling is manifested by the attenuation of the effect of certain electronic operators such as spin−orbit coupling, orbital angular momentum, and the diagonal trigonal field.[20,26,68] The phenomenon may be described very elegantly by the incorporation of vibronic reduction factors (Ham factors), and Ham went on to evaluate the reduction factors using perturbation theory, in the limit where Jahn−Teller coupling is large compared to the perturbing operators. For the systems we are considering, the strength of the Jahn−Teller coupling is small compared to the trigonal field, in which case the zeroth-order functions should be constructed from the degenerate eigenstates of the trigonal field operator.

In the complex trigonal basis, the trigonal field is diagonal and is counter to the Jahn−Teller interaction which is entirely off-diagonal. The effect of Jahn−Teller coupling on the electronic properties of the nondegenerate ground term of the $[V(OH_2)_6]^{3+}$ cation in the β-alums is, in part, quenched by the large trigonal field. The degree of influence is not negligible, however, and the way in which the ground state spin-Hamiltonian parameters are modified may be demonstrated using perturbation theory. In order to keep the problem tractable, we consider only the effect of the mixing-in of the first vibrational excitations of the ^3E_g term into the ground ^3A_g term. Using standard methods of perturbation theory, with the zeroth-order wave functions corresponding to those of $\hat{H}_0 = \hat{H}_{LF+ER} + \hat{H}_{ph}$, and the perturbation defined as $\hat{H}_1 = \hat{H}_{SO} + \hat{H}_{JT}$, the zero-field-splitting of the ground term is found to be

$$D \approx D_{LF} - \frac{A^2\lambda^2\hbar\omega E_{JT}}{(\Delta + \hbar\omega)^3} \approx \frac{(A\lambda)^2(\Delta - A\lambda)}{\Delta(\Delta + A\lambda)} - \frac{A^2\lambda^2\hbar\omega E_{JT}}{(\Delta + \hbar\omega)^3} \quad (17)$$

The parameter, D, is reduced in proportion to E_{JT}. This is because the Jahn−Teller matrix elements are proportional

to $\sqrt{2\hbar\omega E_{JT}}$, and the ground term energies are modified to second-order in the Jahn−Teller interaction. Even when the trigonal field is large, a significant reduction in D can occur when the strength of dynamical Jahn−Teller coupling is modest, as can be ascertained from Figure 2, where D is plotted as a function of E_{JT}. The levels of the ^3A_g-ground term are mixed with states $\Delta + \hbar\omega$ higher in energy. As $\hbar\omega$ appears in both the numerator and the denominator of the second-order correction to the energy, a complicated dependence of D on this parameter is obtained. The value of D is predicted to converge to the ligand field value upon decreasing $\hbar\omega$; i.e. when the vibrational frequency is low, the strong trigonal field effectively decouples the $(^3E_g \oplus {}^3A_g) \otimes e$ Jahn−Teller interaction into $(^3E_g \otimes e) \oplus (^3A_g \otimes e)$ components. This is because the validity of the Born−Oppenheimer approximation rests on the energy separation of electronic states being large compared to the vibrational energy.[25] Upon evaluating the Zeeman interaction as a sequential perturbation to the first-order corrected wave functions of $\hat{H}_0 + \hat{H}_1$, the ground-state g values are calculated as

$$g_{\|} = \frac{g_e - kA\alpha^2 + 2a^2(g_e - kA) + 2b^2(g_e + kA)}{1 + \alpha^2 + 2a^2 + 2b^2} \approx g_e - (g_e + kA)\frac{A^2\lambda^2}{\Delta^2} - \left(\frac{2kA^2\lambda E_{JT}\hbar\omega}{(\Delta + \hbar\omega)^3}\right) \quad (18)$$

where

$$\alpha = \frac{A\lambda}{\Delta} \quad \gamma = \frac{A\lambda}{\Delta + A\lambda} \quad a = \frac{(1/2)\sqrt{\hbar\omega E_{JT}}}{\Delta + \hbar\omega - A\lambda}$$

$$b = \frac{(1/2)\sqrt{\hbar\omega E_{JT}}}{\Delta + \hbar\omega + A\lambda} \quad c = \frac{(1/2)\sqrt{\hbar\omega E_{JT}}}{\Delta + \hbar\omega}$$

$$g_\perp = \frac{[g_e - kA\gamma + g_e\alpha\gamma - kA\alpha + 4ac + 4bc]}{\{(1 + 2\gamma^2 + 4c^2)(1 + \alpha^2 + 2a^2 + 2b^2)\}^{1/2}} \approx g_e - 2Ak\alpha(1 - 4c^2) - \alpha^2(1 + 20c^2) \approx g_e - \frac{2kA^2\lambda}{\Delta}\left(1 - \frac{E_{JT}\hbar\omega}{(\Delta + \hbar\omega)^2}\right) - \frac{A^2\lambda^2}{\Delta^2}\left(1 + \frac{5E_{JT}\hbar\omega}{(\Delta + \hbar\omega)^2}\right) \approx g_e - \frac{2kA^2\lambda}{\Delta}\left(1 - \frac{E_{JT}\hbar\omega}{(\Delta + \hbar\omega)^2}\right) \quad (19)$$

Plots of the principal g values versus E_{JT} are shown in Figure 2. The anisotropy of the **g**-matrix is predicted to decrease as a linear function of E_{JT}, although the modification from the values obtained from ligand field theory is slight.

Also shown in Figure 2 are the same quantities calculated numerically, using the same $^3T_{1g}$(F, P) electronic basis. The numerical calculations provide confirmation that the expressions for the spin-Hamiltonian parameters, formulated using perturbation theory, are qualitatively correct. A larger basis set is employed, and hence, the deviation of the spin-Hamiltonian parameters from the values arising from ligand field theory is more pronounced. The variation of D, $g_{\|}$, and $g_\perp$ with E_{JT} remains linear, and the attenuation of the zero-field-splitting is significant.

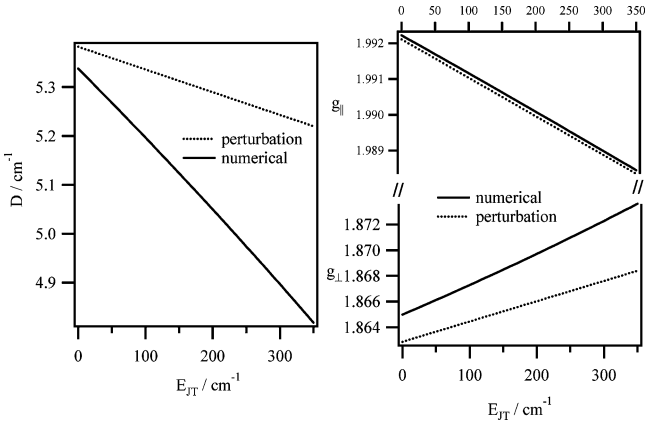

Figure 2. Dependencies of the ground-state spin-Hamiltonian parameters of an octahedrally coordinated d^2 complex on the Jahn−Teller stabilization energy. The values displayed with the broken line marked "perturbation" were calculated using the expressions given in eqs 17−19. Those indicated by the solid line were calculated by numerical diagonalization of the vibronic Hamiltonian. Both sets of calculations employ the $^3T_1$(F, P) electronic basis given in Table 1 with the following parameters common to both sets of calculations: $\Delta = 1918$ cm^{-1}, $\lambda = 76$ cm^{-1}, $A = 1.414$, $\hbar\omega = 900$ cm^{-1}, and $k = 0.88$.

The way in which the electronic properties are modified can be understood in the spirit of the theory of Ham.[26] Defining three reduction factors p_Δ, p_λ, and p_k which multiply Δ, λ, and k, respectively, and equating the spin-Hamiltonian parameters calculated using eqs 15 and 16 with those calculated numerically yields the relations plotted in Figure 3. The expressions p_λ and p_k both multiply orbital angular momentum operators and have approximately the same value, which we shall designate p_L. p_Δ multiplies the term for the trigonal field splitting and reflects the mixing-in of vibronic states from the higher lying ^3E_g term, through the Jahn−Teller interaction. When $E_{JT} = 350$ cm^{-1}, $p_\Delta \sim 3/5$, $p_L \sim 3/4$, betokening a significant quenching of the effects of the orbital operators. In the limit where $\Delta \gg \lambda$, and $(\Delta + h\omega) \gg A_1$, we obtain

$$D \approx D_{LF}\frac{{p_L}^2}{p_\Delta} \quad (20)$$

where

$$\frac{{p_L}^2}{p_\Delta} \approx \left(1 - \frac{\Delta E_{JT}\hbar\omega}{(\Delta + \hbar\omega)^3}\right) \quad (21)$$

When the perturbation calculation is taken to higher-order, the expressions corresponding to the vibronic reduction of both D, and the orbital contribution to $g_\perp$, should converge, as both these quantities are reduced by $\sim {p_L}^2/p_\Delta$ in the limit $\Delta \gg \lambda$.

Numerical calculations employing all 45 states of the d^2 configuration yield results similar to those presented in Figure 2. Using the parameters given at the end of section 4.1 as input, D decreases linearly from 5.3162 to 4.7913 cm^{-1} on increasing E_{JT} from 0 to 350 cm^{-1}. Likewise, the principal g-values converge, with $g_{||}$ decreasing linearly from 1.9527 to 1.9509, and $g_\perp$ increasing from 1.8591 to 1.8669. The spin-Hamiltonian parameters tend toward the ligand field

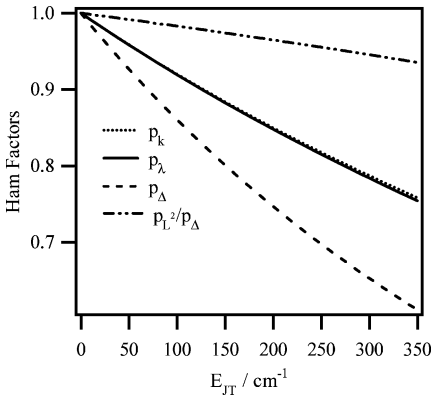

Figure 3. Variation of the Ham factors, describing the effect of dynamical Jahn−Teller coupling on the magnetic response of the ^3A_g (S_6) ground term, as a function of E_{JT}. The vibrational frequency and ligand field parameters are identical to those given in the caption of Figure 2.

values, as the phonon frequency is decreased. In the preceding paper, it was shown that the ground-state spin-Hamiltonian parameters of the $[V(OH_2)_6]^{3+}$ cation change dramatically upon deuteriation, with D decreasing and $g_{||}$ increasing. These calculations show that the isotope effect cannot be due to dynamical Jahn−Teller coupling, although the effect must be included if a rigorous definition of the electronic structure is sought.

4.3. Effect of Jahn−Teller Coupling on the $^3A_g \rightarrow {}^3E_g$ Electronic Raman Profile. When the ^3E_g term is perturbed sequentially by Jahn−Teller and spin−orbit coupling, the energy spacing between the three sets of spinor levels is given by $p_L^E A\lambda$ where p_L^E diminishes from unity as an exponential function of $E_{JT}/\hbar\omega$.[20,68] Recently, we communicated the 15 K electronic Raman spectrum arising from the $[V(OH_2)_6]^{3+}$ cation in GuVSH, in which the transitions to the higher-lying ^3E_g term were highly resolved.[69] The energy range spanned by the spinor levels was found to be significantly lower than any reasonable estimate of $2A\lambda$. The spectrum affords an archetypal example of Ham quenching, and further details shall be presented in a future publication. The electronic Raman spectra of $[V(OH_2)_6]^{3+}$ in hydrogenous and deuterated samples of the rubidium vanadium sulfate β-alums are shown in Figure 4. The spectra are reproduced from an earlier publication in which an attempt was made to model the electronic Raman profiles within the confines of ligand field theory.[16] A pronounced reduction in the bandwidth of the $^3A_g \rightarrow {}^3E_g$ transition is seen to occur upon deuteriation. The data are perplexing, in that the electronic Raman profile of the protonated and deuterated salts spans an energy range which is, respectively, greater and less than that expected from ligand field theory. It is unlikely lifetime broadening is the determining factor, as the profiles exhibit extensive structure, and the bandwidths change little in the temperature range 80−200 K. A vibronic coupling mechanism involving the librational modes of water coordinated to vanadium(III) is implicated, as the energies of these vibrations diminish by $\sim(1/\sqrt{2})$ upon deuteriation, but the anomalously large bandwidth of the hydrogenous salt cannot be explained with the first-order perturbation theory of Ham, as a reduction in the energy spacing of the spinor levels, on

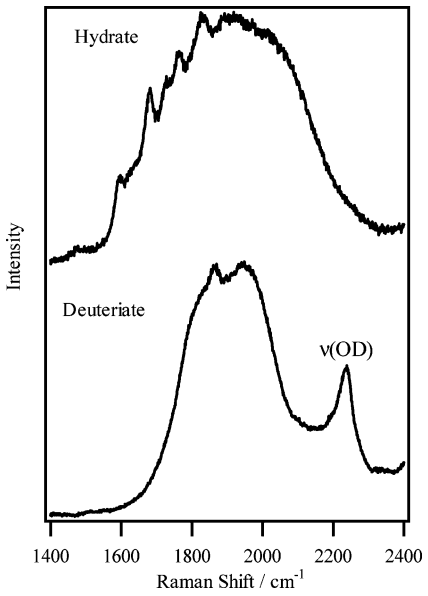

Figure 4. Electronic Raman spectra of hydrogenous and deuterated $Rb[V(OH_2)_6](SO_4)_2 \cdot 6H_2O$, reproduced from ref 16. The broad band centered at ~1930 cm^{-1} has been assigned to the transitions depicted in Figure 1b. The band at ~2200 cm^{-1} in the deuterated salt has been assigned as an O−D stretching vibration.

account of Jahn−Teller coupling, is always predicted.[26] When the calculation is taken to second order, terms appear linking the spinor levels of the ^3E_g term with overtones of the ^3A_g ground-term. Thus, overtones of Jahn−Teller active vibrations, as well as higher harmonics, may obtain significant intensity when occurring in the proximity of the electronic Raman band.

The effect of Jahn−Teller coupling on the profile of the electronic Raman transition is aptly illustrated by numerical calculations. As before, parameters are chosen that roughly describe the $[V(OH_2)_6]^{3+}$ cation in the β-alums. The variation of the energies of the low-lying vibronic states with E_{JT} is shown in Figure 5 by means of solid lines ($n = 0$ at $E_{JT} = 0$) or broken lines ($n \neq 0$ at $E_{JT} = 0$). An energy frame is shown that encompasses the nine states of the $^3T_{1g}$ electronic ground term ($n = 0$), and the first two vibrational excitations ($n = 1, 2$) of the ^3A_g ground term, with $\hbar\omega$ set to 900 cm^{-1}; the energy of the ground state is set to zero.

In the vibronic subspace, the six spinor levels of the ^3E_g term transform the same way as the six states comprising the first vibrational excitations of the ^3A_g ground term. The mixing that then occurs upon increasing Jahn−Teller coupling strength leads to a depression of the vibrational excitations, and contributes to an increase in the energies of the states approximating to the zero-phonon levels of the ^3E_g term, relative to the ground term, as shown in Figure 5. The energies of the second- and third-harmonics are similarly depressed. With $E_{JT} = 350$ cm^{-1}, the spacing of the levels of the ^3E_g term is ca. 70% of $2A\lambda$, in accordance with the theory of Ham.[26]

In Figure 6 is shown the calculated electronic Raman cross-section as a function of E_{JT}, between 1400 and 2400 cm^{-1}. The vibronic sidebands that occur in this spectral region are due to the second term in the Jahn−Teller Hamiltonian, given in eq 5, that mixes the levels of the ^3A_g

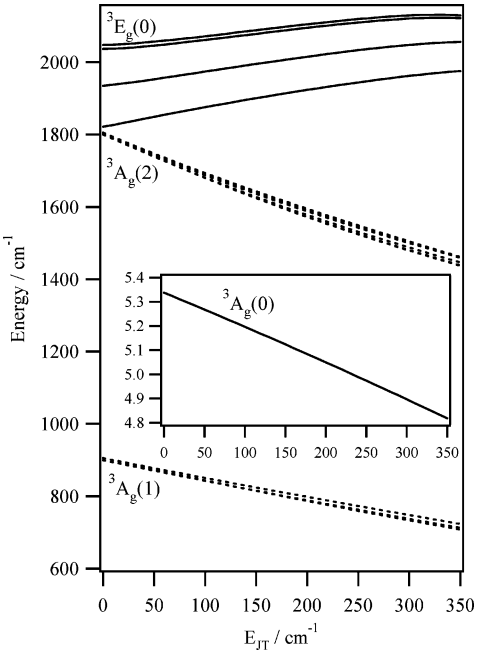

Figure 5. Variation of the energies of the low-lying vibronic states of an octahedrally coordinated d^2 system as a function of E_{JT}: $\Delta = 1918$ cm^{-1}, $\lambda = 76$ cm^{-1}, $A = 1.414$, $\hbar\omega = 900$ cm^{-1}. The axis labels are common to both the main figure and the insert. The symmetry labels relate to the makeup of the states with $E_{JT} = 0$. Solid lines denote the ground vibrational states of the trigonal components of the $^3T_{1g}$ ground term ($(^3A_g(0), {}^3E_g(0))$); broken lines denote the first and second vibrational excitations of the ^3A_g ground term ($(^3A_g(1), {}^3A_g(2))$).

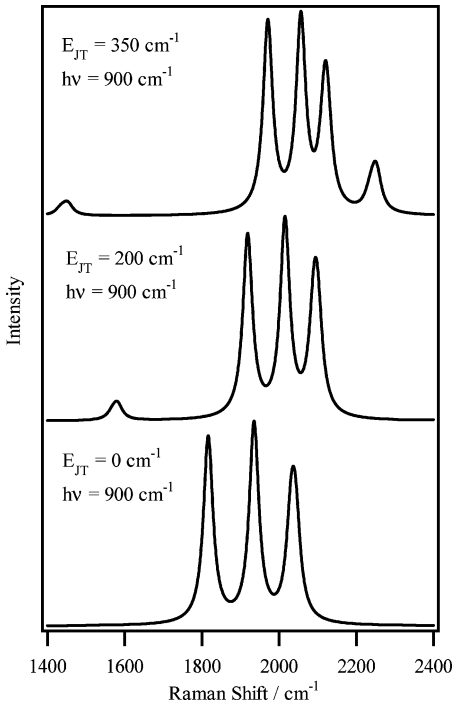

Figure 6. Theoretical electronic Raman profiles as a function of E_{JT} calculated using the parameters given in the caption of Figure 5.

and ^3E_g trigonal terms. Figure 7 demonstrates the effect on the vibronic energy levels of decreasing the vibrational energy for a constant value of E_{JT}. As the vibrational frequency is decreased while holding E_{JT} constant at 350 cm^{-1}, there occurs an avoided level crossing of vibronic states, as the third vibrational excitations of the ^3A_g ground

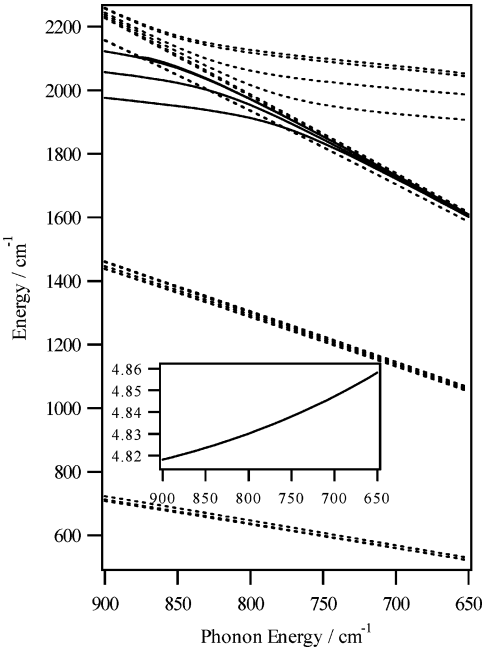

Figure 7. Variation of the energies of the low-lying vibronic states of an octahedrally coordinated d^2 system as a function of $\hbar\omega$: $E_{JT} = 350$ cm^{-1}, $\Delta = 1918$ cm^{-1}, $\lambda = 76$ cm^{-1}, and $A = 1.414$. The axis labels are common to both the main figure and the insert.

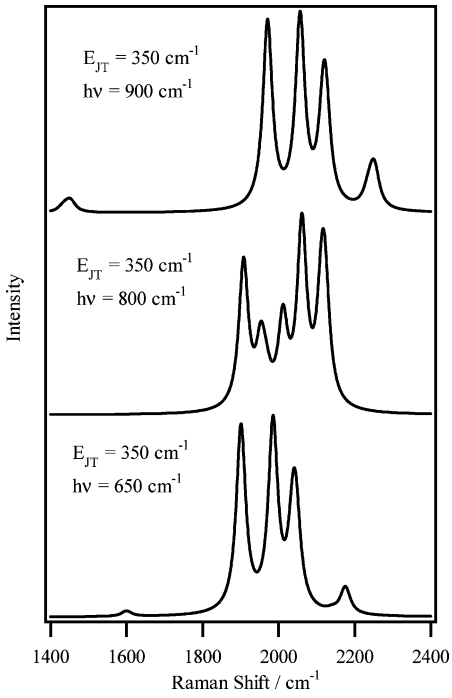

Figure 8. Theoretical electronic Raman profiles as a function of $\hbar\omega$ calculated using the parameters given in the caption of Figure 5.

term approach the levels of the ^3E_g term. With $\hbar\omega$ set to 800 cm^{-1}, the calculated electronic Raman band in Figure 8 is broad and structured and bears little resemblance to the profile calculated using ligand field theory, shown in Figure 6; as $\hbar\omega$ is reduced further, the familiar ^3E_g pattern re-emerges.

These theoretical profiles are calculated from a single-mode model, when in reality the librational modes of water coordinated to vanadium(III) are strongly coupled in the

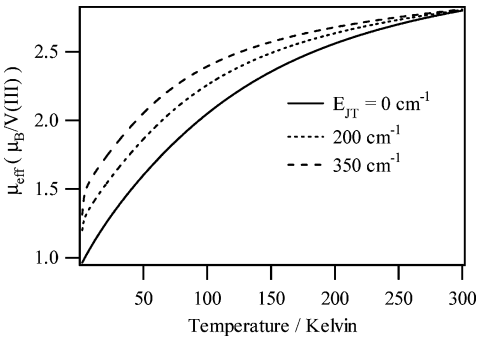

Figure 9. Plot of μ_{eff} vs temperature for a vanadium(III) cation subject to a cubic field, and dynamical Jahn−Teller coupling. The parameters are the same as those given in the caption of Figure 2, with the trigonal field set to zero, and for various values of E_{JT} shown on the figure.

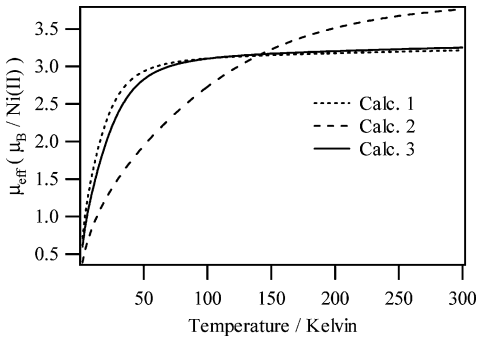

Figure 10. Theoretical values of μ_{eff} vs temperature. The curve designated "Calc. 1" was computed with the parameters $\Delta = 845$ cm^{-1}, $\lambda = -130$ cm^{-1}, $A = 1.5$, and $k = 0.55$. The following parameters are common to calculations 2 and 3: $\Delta = 0$ cm^{-1}, $\lambda = -252$ cm^{-1}, $A = 1.5$, and $k = 0.8$. For Calc. 2, the Jahn−Teller interaction was set to zero. For Calc. 3, $\hbar\omega$ and E_{JT} were set to 300 and 1000 cm^{-1}, respectively.

β-alums, with energies spanning ∼750−950 cm^{-1}; it is found that the energy of no single librational mode is depressed by as much as predicted from these calculations.[70] Significant coupling to a low-energy lattice mode is also to be expected.[46] Therefore, the parameters pertaining to the vibronic interaction, used to generate the foregoing figures, should not be overemphasized. In the hydrogenous salt, there are a host of overtone and combination bands, involving the librational modes of water coordinated to vanadium(III), occurring in the proximity of the electronic Raman band. The enhancement of the e_g components of these bands, through the Jahn−Teller interaction, provides a plausible explanation for the anomalous bandwidth of the electronic Raman profile.

4.4. Effect of Dynamical Jahn−Teller Coupling on the Temperature Dependence of the Magnetic Susceptibility Arising from $^3T_1$ Terms. In cubic symmetry, the nine levels of the $^3T_{1g}$ ground term are split by spin−orbit coupling into three sets of levels that may be specified by the total angular momentum quantum number J. For hexacoordinate d^2 complexes, the $J = 2$ state is lower lying, with the $J = 1$ and $J = 0$ levels $2A\lambda$ and $3A\lambda$ higher in energy, respectively. The variation of the effective magnetic moment with temperature is shown in Figure 9 for the $[V(OH_2)_6]^{3+}$ cation, employing the same parameters given previously, but setting Δ to zero. The moment decreases gradually with temperature, reflecting the depopulation of the $J = 1$ state. Also shown in Figure 9 are plots of μ_{eff} versus T, as a function of E_{JT}. The magnetic properties of the $[V(OH_2)_6]^{3+}$ cation, under the influence of dynamical Jahn−Teller coupling, are in many ways akin to those of the $[Ti(OH_2)_6]^{3+}$ cation, discussed in depth previously.[46−48] Jahn−Teller coupling gives rise to an effective quenching of spin−orbit coupling and orbital angular momentum,[20] resulting in a shallower decrease in μ_{eff} upon decreasing temperature, and a greater moment at $T = 0$ K. The electronic properties are not lost, however, but are simply redistributed to other vibronic states and recovered when these states are thermally occupied. Therefore, μ_{eff} approaches the same asymptotic values, irrespective of the coupling strength. The theoretical curves were calculated with the rather large vibrational energy of 900 cm^{-1}. The effect of Jahn−Teller coupling intensifies approximately in proportion to the ratio $E_{JT}/\hbar\omega$, to the point where $\hbar\omega \sim \lambda$.[46]

In the majority of the crystal systems of which the authors are aware, the vanadium(III) cation is subject to a strong trigonal field, resulting in a ^3A_g (S_6) ground term. It seems an inexplicable quirk of nature that the nondegenerate trigonal component is always found lower lying. In instances where $\Delta \gg k_BT$, it is common to model the data using the spin-Hamiltonian given in eq 11, adding $W^{(2)}B^2$ to the terms along the diagonal, where $W^{(2)}$ is the second-order Zeeman coefficient. From ligand field theory, we obtain $W_z^{(2)} = 0$, $W_\perp{}^{(2)} \approx -k^2A^2/\Delta$, in the limit $\Delta \gg \lambda$. As a consequence of the Jahn−Teller effect, $W_\perp{}^{(2)}$ is reduced by $\sim p_L{}^2/p_\Delta$. When $\Delta \gg k_BT$, the difference between susceptibility curves calculated using the $S = 1$ spin-Hamiltonian and those using the full vibronic Hamiltonian is very slight. If, however, the ground-state spin-Hamiltonian parameters are interpreted without due regard to dynamical Jahn−Teller coupling, then the values of Δ and λ so inferred could be quite misleading.

Susceptibility curves relevant to tetrahedral nickel(II) complexes may be generated by reversing the sign of λ. Though not the advertised topic of this paper, the reader will forgive the digression. The t_{2g} orbitals now participate in σ-bonding, and hence, the Jahn−Teller interaction is stronger. In addition, the splitting of the states of the $^3T_{1g}$ term by spin−orbit coupling is commonly comparable to that by low symmetry ligand fields, in which case an analysis of the magnetism in the formalism of the $S = 1$ spin-Hamiltonian is not appropriate. Susceptibility data for a range of tetrahedral nickel(II) complexes have been obtained in the range 80−300 K and modeled using the ligand field Hamiltonian matrix, given in Table 1.[67] The values of the spin−orbit coupling parameter derived are typically 0.4−0.6 of the free ion value, implying significant delocalization of the unpaired electron density onto the ligand. We have found that these data can be satisfactorily reproduced choosing much higher values of λ, when dynamical Jahn−Teller coupling is included. As an example, consider Figure 10, where theoretical plots of μ_{eff} versus T are presented. The curve designated "Calc. 1" was computed using the following parameters, $\Delta = 845$ cm^{-1}, $\lambda = -130$ cm^{-1}, $A =$

(70) Best, S. P.; Armstrong, R. S.; Beattie, J. K. *J. Chem. Soc., Dalton Trans.* **1992**, 299.

1.5, and $k = 0.55$. For "Calc. 2", we have set the trigonal field to zero, and increased k and λ to 0.8 and -252 cm^{-1}, respectively, giving rise to a very different curve of μ_{eff} versus temperature. When dynamical Jahn−Teller coupling is included, curve "Calc. 3" is generated, which closely resembles "Calc. 1". On the basis of these results, the parameters derived from ligand field analyses are of doubtful significance, when not accompanied by spectroscopic measurements. Calc. 1 uses parameters orginally employed to model susceptibility data for the $(Ph_3P)_2NiCl_2$ complex. Since then, magnetic data have been obtained over a wider temperature range and interpreted along with optical and HFEPR data, in the framework of the AOM.[11] For this system, the axial field is in fact $\sim$4000 cm^{-1}. The effect of dynamic Jahn−Teller coupling on the ground-state spin-Hamiltonian parameters is then negligible.

5. Summary and Conclusions

The zero-field-splitting of the ^3A_g (S_6) ground term of the $[V(OH_2)_6]^{3+}$ cation is reduced significantly by dynamical Jahn−Teller coupling. In the β-alums, where the trigonal field is large, the reduction in the parameter D is estimated to be $\sim$10%. The quenching is predicted to be most pronounced in complexes where the trigonal field is moderate, the metal−ligand π-bonding is anisotropic, and the energies of the Jahn−Teller active vibrations are of the order of the trigonal field. In ignoring dynamical Jahn−Teller coupling, the ligand field analysis of the $[V(OH_2)_6]^{3+}$ cation, presented in the previous paper, underestimates the true value of the spin−orbit coupling parameter, and absorbs the small modification of the g-values into the orbital reduction factors. The calculations presented in this work also provide a plausible explanation for the anomalous profile of the $^3A_g \rightarrow {}^3E_g$ (S_6) electronic Raman transition electronic Raman band in the vanadium alums, whereby overtones of Jahn−Teller active vibrations may have their intensity enhanced, when occurring in the vicinity of the electronic transition. The calculations do not render an explanation for the effect of isotopic substitution on the ground-state spin-Hamiltonian parameters. A slight increase in D is predicted upon deuteriation on account of vibronic coupling, when in fact a rather significant decrease is observed. This result leads us to conclude that the quantity $(A\lambda)^2/\Delta$ decreases in magnitude upon deuteriation. Pronounced changes in the structure and bonding of transition metal hydrates upon deuteriation are not uncommon but are poorly understood.[71] We hope that the observed isotope effect stimulates further theoretical work in this area.

Though the calculations were undertaken with the $[V(OH_2)_6]^{3+}$ cation in mind, the methodology is equally applicable to any transition metal complex with an orbital triplet ground term, subject to an axial distortion, common examples being hexacoordinate iron(II) and tetrahedral nickel(II) complexes. The use of angular overlap model matrices to construct the vibronic Hamiltonian affords an "inorganic-chemist" friendly approach to conducting vibronic coupling calculations, incorporating all the ligand field states, with minimal parametrization.

The common perception of Jahn−Teller coupling is that it is a symmetry lowering mechanism and is of consideration only for transition metal complexes with orbital doublet ground terms. However, as we have shown, the magnetic properties of complexes with orbital triplet ground terms may be modified substantially when Jahn−Teller and spin−orbit coupling are of comparable magnitudes. Though the degree of Jahn−Teller coupling is not strong enough to bring about a pronounced distortion, and though the orbital degeneracy may be lifted by an axial field, the phenomenon must still be considered when a precise description of the electronic structure is sought.

Acknowledgment. We thank Joshua Telser for invaluable comments regarding the magnetism of tetrahedrally coordinated nickel(II) complexes. This work was funded by the Swiss National Science Foundation.

Supporting Information Available: File containing the derivation of eqs 17−19. This material is available free of charge via the Internet at http://pubs.acs.org.

IC049291T

(71) Dobe, C.; Carver, G.; Tregenna-Piggott, P. L. W.; McIntyre, G. J.; Augustyniak-Jablokow, M. A.; Riley, M. J. *Inorg. Chem.* **2003**, *42*, 8524.